https://doi.org/10.30799/jacs.280.26120501 J. Adv. Chem. Sci. – Volume 12 Issue 5 (2026) 1021–1029

Share Your Innovations through JACS Directory

Journal of Advanced Chemical Sciences

Visit Journal at https://www.jacsdirectory.com/jacs

ISSN: 2394-5311

Development of Benzo[b]thiophene Linked-Oxadiazole Derivatives for Potential Antimicrobial and Anti-TB Targets: Evaluation of ADME-Tox and *In-silico* Docking

Nagaraju Madala[1,2], Vishal Sharma[3,*], Srilalitha Vinnakota[4]

[1]*Centre for Chemical Sciences and Technology, University College of Engineering Science and Technology, Jawaharlal Nehru Technological University, Hyderabad – 500 085, Telangana, India.*
[2]*Medicinal Chemistry Division, VSN LABS, IDA Cherlapally, Phase-V, Hyderabad – 500 051, Telangana, India.*
[3]*Discovery Chemistry Division, Jubilant Biosys Ltd, Knowledge Park II, Greater Noida – 201 306, Uttar Pradesh, India.*
[4]*Dept. of Chemistry, Faculty of Science and Technology, ICFAI Foundation for Higher Education, Dontanpally, Hyderabad – 501 203, Telangana, India.*

ARTICLEDETAILS

Article history:
Received 02 June 2026
Accepted 19 June 2026
Available online 16 July 2026

Keywords:
Benzo[*b*]thiophene
1,2,4-Oxadiazole
1,3,4-Oxadiazole
Anti-TB
Antimicrobial
Computational Studies

ABSTRACT

The present work reports the synthesis of new *bis*-oxadiazole-bearing benzo[*b*]thiophene derivatives as well as assessments of their antimicrobial and antitubercular activity through both *in vitro* and *in silico* approaches. The novel benzo[*b*]thiophene-based oxadiazole derivatives (**7a**–**7k**) were synthesized *via* a three-step path involving the preparation of thioacetonitrile, followed by the conversion to acetimidamide, and finally cyclization with various functionalized benzoic acids. The structural elucidation of the prepared benzo[*b*]thiophene compounds was established by ^{1}H-NMR, ^{13}C-NMR, and HRMS spectroscopic analysis. *In vitro* antimicrobial activity against Gram-(–ve), Gram(+ve) and fungal microorganisms and antitubercular effect on the H_{37}Rv strain were assessed for each synthesized compound. It was revealed that compound **7f** showed well-established antibacterial affinities on *S. aureus* and *P. aeruginosa* with zones of inhibition of 39.95±0.82 and 37.29±0.33 mm in comparison to the reference drug gemifloxacin (37.02±0.92 and 36.10±2.17 mm). Notably, compounds **7c** and **7h** displayed the highest antifungal activity among the tested compounds, with selectivity towards the *C. albicans* ZI values of 30.15±0.28 and 31.37±1.32 mm, with respects to CLZ (ZI = 29.36±1.15 mm). Among them, oxadiazole conjugates **7a** (MIC = 5.80 µM), **7f** (2.89 µM), and **7h** (3.10 µM) showed potent anti-TB activity on the tested H_{37}Rv compared to the conventional drug STM. Moreover, *in silico* molecular docking studies indicate that these conjugates strongly interrelate and bind with the *C. albicans* and *M. tuberculosis* active sites (PDB codes: 5FSA & 4FDN). Compound **7c** showed the best docking score (−11.77 kcal/mol), followed by ligand **7f** (−10.68 kcal/mol), with key H-bond interacting residues such as Gly^{77}(A), Ser^{79}(A), Arg^{78}(A), Thr^{142}(A), and Tyr^{435}(A). Additionally, the synthesized compounds were screened for drug-likeness based on Lipinski's rule of five and ADME-Tox parameters. Overall, the study identifies promising oxadiazole-based inhibitors and provides a valuable insight for further optimization and development of potential antimicrobial targets.

1. Introduction

Tuberculosis (TB) is one of the contagious, highly fatal, and pervasive respiratory infections caused by the gram-positive bacteria *Mycobacterium tuberculosis* (Mtb) [1]. Recent years have seen the resurgence of tuberculosis as a significant worldwide health issue, especially during the COVID-19 epidemic, which significantly hinders people in need of long-term care [2]. A major increase in the number of multiple drug-resistant (MDR-TB) and extremely drug-resistant (XDR-TB) cases, as well as the co-occurrence of TB with HIV infection and atypical mycobacterial infections, is the main cause of the substantial rise in infection and mortality rates during this pandemic, according to the World Health Organization's (WHO) report on TB. Despite these considerations, the development of MDR-TB makes TB therapy difficult [3]. Approximately 10 million people worldwide suffer from the illness, and 1.5 million of them die from it every year [4]. According to the WHO 2022 report, there were more than 1.4 million TB-related fatalities and more than 0.18 million HIV-TB coinfection-related deaths [5]. It is estimated that 1.7 billion people, or 23% of the global population, have a latent TB infection and are therefore at risk of contracting active disease at some point in their lives. Current anti-TB medications, such as isoniazid, ethambutol, ethionamide, and cycloserine, concentrate on inhibiting the cell wall-forming processes, whereas other medications, such as rifampicin, streptomycin, capreomycin, and linezolid, target distinct protein-making processes to prevent the mycobacterium's growth and spread [6].

Bacteria are microorganisms that significantly impact human health. They have an impact on the development of a variety of diseases and illnesses, ranging from minor conditions like pharyngitis and urinary tract infections to more severe and potentially lethal conditions like meningitis and pneumonia [7]. Bacterial toxins can damage organs and tissues, resulting in chronic health difficulties [8]. Antimicrobial resistance (AMR), which has been exacerbated by the COVID-19 pandemic, has posed a serious danger to public health and global economic development [9]. According to a WHO report, antibiotic resistance has made it more challenging to treat and control bacterial diseases. An estimated 1.27 million fatalities and disability-adjusted life years are attributed to antimicrobial-resistant bacteria each year [10]. Therefore, there is an urgent need to create new antimicrobial medicines, especially those that fight Gram-negative bacteria [11]. Thankfully, other antibiotics have been approved for commercial use through structural modification of tetracyclines, quinolones, aminoglycosides, and other compounds, such as plazomicin, delafloxacin, moxifloxacin, and gemifloxacin. At the same time, certain natural antibacterial compounds have been the subject of clinical studies [12]. Fungal infections have also emerged as a growing threat to human health in recent years [13]. While there are several reasons for this, the increase in HIV-positive patients and the number of cancer patients undergoing chemotherapy are two important ones [14]. As a result, researchers are now looking for novel molecular targets for antifungal drugs. Some patients still have innate or acquired antifungal resistance, despite the fact that many new antifungal drugs have been introduced in the last five years. Additionally, several recently developed antifungal drugs have substantial negative effects. Therefore, there is a continuing

*Corresponding Author:naga@vsnlabs.in(Vishal Sharma)

https://doi.org/10.30799/jacs.280.26120501

need for new antifungal drugs that can specifically target fungus without interfering with the metabolic functions of the host.

The most significant traditional area of organic chemistry is heterocycles, and because of their industrial, antimicrobial, and medical uses, heterocycles are gaining more attention in research [15]. Numerous natural compounds, including as DNA, RNA, chlorophyll, hemoglobin, vitamins, and others, are formed in large part by the heterocyclic ring [16]. Numerous heterocycles are also the building blocks of proteins and other chemicals that comprise the body's structure, including the vital amino acid proline, the pigment chlorophyll, which is involved in photosynthetic processes, and the pigment hemoglobin, which transports oxygen [17]. Heterocyclic components are found in a number of substances, primarily of natural origin, including alkaloids, morphine, vinblastine, and reserpine, as well as a range of antibiotics, including cephalosporin, penicillin, and others [18]. Because of its many biological activities and drug-like properties, benzo[*b*]thiophene is a potentially intriguing and practical pharmacophore to study.

Numerous pharmaceutical substances, such as zileuton, sertaconazole, and raloxifene, as well as naturally occurring chemical molecules, include these fundamental structures. Many biological actions, such as antitubercular [19], antimicrobial [20], antifungal [21], antioxidant and anti-inflammatory [22], anticonvulsant [23], anticancer [24], and antidepressant [25], are exhibited by benzo[b]thiophenes. From the standpoint of target-based drug design and medicinal chemistry, functional derivatives of the 1,2,4-oxadiazole ring are a special class of organic molecules. Indeed, compounds with the 1,2,4-oxadiazole moiety have several beneficial biological properties, such as antibacterial [26] and antimycobacterial [27], antifungal [28], antiproliferative [29], anti-inflammatory [30], antiparasitic [31], antiviral, anti-infective, in general [32], and other activities. The 1,2,4–oxadiazole fragment is also known to be a building block for the synthesis of novel high-energy materials.

1,3,4-oxadiazoles are nitrogen-containing heterocyclic compounds with significant pharmacokinetic properties and lipophilicity that may influence the drug's ability to permeate across membranes and reach the target. Because of their many biological actions, including anticancer [34], anti-tubercular [35], antibacterial, antifungal [36], antihypertensive, antiviral, antioxidant, anti-inflammatory, and antidiabetic, 1,3,4-oxadiazole compounds are regarded as one of the most important moieties [37]. Excellent pharmacological actions are more likely to be caused by the linkage of -N=C-O- in the 1,3,4-oxadiazole ring structure [38]. Nesapidil, Zibotentan, Tiodazosin, Fenadiazole, Raltegravir, Pleconaril, Butalamine, Libexin, Fasiplon, and Arzoxifene are only a few of the many commercially licensed medications that include 1,3,4-oxadiazole, 1,2,4-oxadiazole, and a benzo[*b*]thiophene ring (Chart 1) [39]. Motivated by these discoveries, the present work centres on the synthesis, using hybridization and bioisosteric modification procedures, of three kinds of heterocyclic motifs *via* 1,3,4–oxadiazole, 1,2,4–oxadiazole substituted benzo[*b*]thiophene. A molecular docking study was conducted to examine these compounds' possible interactions with verified antibacterial and tuberculosis targets in order to further promote their development.

This present work targeted important bacterial and tuberculosis enzymes with the PDB codes 5FSA and 4FDN in order to obtain more evidence and confirmation of the in vitro antibacterial activities we saw in our benzo[*b*]thiophene derivatives. To forecast their pharmacokinetic behavior and toxicity profiles, an in-silico Absorption, Distribution, Metabolism, Excretion, and Toxicity (ADMET) analysis was also carried out.

Important characteristics, including as solubility, lipophilicity, intestinal absorption, metabolic stability, clearance, and toxicity risks, were assessed to determine their safety and drug-likeness. The results offer valuable insights into their mechanisms of action, pharmacokinetic behaviour, and potential limitations, thereby laying a solid foundation for their further development as effective and sustainable therapeutic candidates.

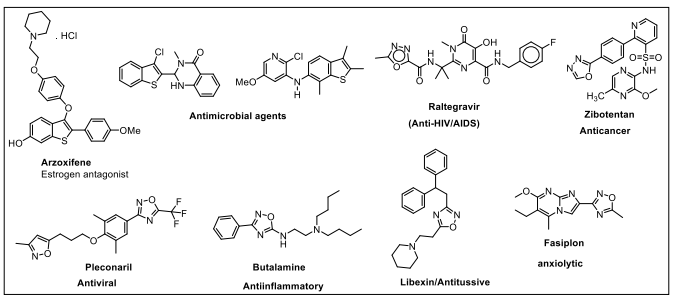

Chart 1 Commercially available drugs containing benzo[*b*]thiophene, 1,3,4-oxadiazole & 1,2,4-oxadiazole

2. Results and Discussion

2.1 Synthesis and Characterization

Therefore, as part of our on-going research effort on the synthesis of novel bioactive heterocycles [40-42], we are very much engrossed in the design and synthesis of the title compounds. Firstly, cyclisation of 1-(2-chlorophenyl)ethan-1-one group (**1**) with methyl 2-mercaptoacetate by stirring it with NaH in DMF for 3 h followed by dilution with ethyl acetate and washing with water and brine solution. Hydrazones (**3**) was prepared in the second step by refluxing with methyl 3-methylbenzo[*b*]thiophene-2-carboxylate (**2**) in presence of ethanol for 6 h. Finally, cyclisation of hydrazones with carbon disulphide and potassium hydroxide in the presence of ethanol for 7 h, followed by washing with ethyl acetate in a vacuum under pressure (Scheme 1). Monitoring of the reaction was done by thin layer chromatography and completion of reaction was confirmed by single spot in TLC under UV lamp. As seen in Scheme 2, the 1,3,4-oxadiazole-2-thiol was subsequently transformed into acetonitrile (**5**) while being exposed to 2-bromoacetonitrile, potassium carbonate, and acetone at reflux temperature for six hours. To prepare acetimidamide product (**6**) from 1,3,4-oxadiazol-2-thioacetonitrile (**5**) with hydroxyl amine hydrochloride in dichloromethane as the solvent with a base catalytic amount of triethyl amine at rt for 10 h. The second strategy is for the synthesis of compound **7a–7k** was produced through the reaction of O-acylation and cyclization steps were conducted in a one-pot reaction with the corresponding acids in the presence of coupling reagent EDC.HCl. Next, oxadiazoles **7a–7k** were obtained through reflux of the acylated intermediate in ethanol and in the presence of sodium acetate for 4-5 h (Scheme 2) [43]. All the compounds **7a-7k** were obtained in moderate to be good yields and the structures of all compounds **7a-7k** were confirmed by their spectroscopic data.

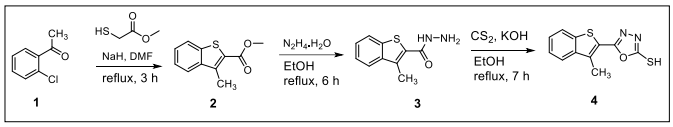

Scheme 1 Preparation of intermediate benzo[*b*]thiophene with 1,3,4-oxadiazole **5**

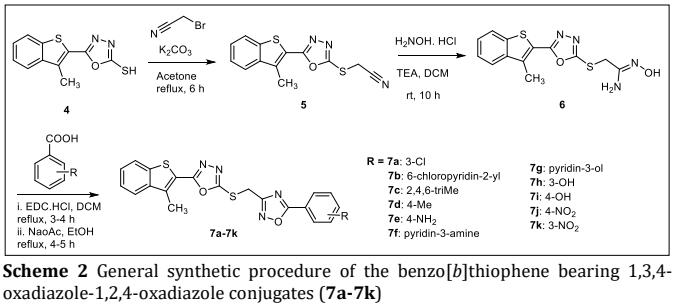

Scheme 2 General synthetic procedure of the benzo[*b*]thiophene bearing 1,3,4-oxadiazole-1,2,4-oxadiazole conjugates (**7a-7k**)

Evaluation of the structure of novel derivatives was confirmed by spectroscopic methods such as ^{1}H-NMR, ^{13}C-NMR, and mass analysis. Derivatisation was confirmed by the disappearance of peaks of amine (NH_2) and OH at 3345.23 and 3424.68 cm^{-1} of acetimidamide and the appearance of C=N and C=C at 1446.35 and 1603.25 cm^{-1} in compound **7a**. Moreover, the peaks of COC and CSC linkers at 1167.28 and 1254.58 cm^{-1} in compound **7a** also confirmed the formation of oxadiazole. IR spectra peaks of sp^2 (=CH) and sp^3 (CH) functional groups were found at 3067.89 and 2846.28 cm^{-1} in the **7a** derivative. In addition, the ^{1}H-NMR of compound **7a** recorded a singlet signal at δ 2.27 ppm for the benzo[*b*]thiophene methyl group and a 4.57 ppm singlet for one *S*-methylene proton, in addition to one doublet and triplet signals at 7.61 and 7.83 ppm for benzo[*b*]thiophene protons, respectively. ^{1}H-NMR (multiplet) peaks at 7.42–7.52 ppm indicated the four aromatic protons. ^{13}C-NMR peaks at 176.25 and 162.46 ppm indicated the 1,2,4-oxadiazole carbons, whereas the other resonance peaks showed for 1,3,4-oxadiazole carbons at 159.23 and 143.51 ppm, respectively. Moreover, the resonance signals at δ 141.18 and 119.64 ppm indicated the formation of aromatic linkers in compound **7a**. In the ^{13}C-NMR signal, *S*-methylene and benzo[*b*]thiophene carbons exhibited at δ 35.48 and 15.82 ppm for compound **7a**. Besides, its HRMS spectrum revealed a molecular ion peak at *m/z*=441.0310 (100%) for the compound 5-(3-chlorophenyl)-3-(((5-(3-methylbenzo[*b*]thiophen-2-yl)-1,3,4-oxadiazol-2-yl)thio)methyl)-1,2,4-oxadiazole (**7a**). Additionally, the elemental analysis and mass spectrometric data were also found in conformity with the compound's characterization.

https://doi.org/10.30799/jacs.280.26120501

Cite this Article as: Nagaraju Madala, Vishal Sharma, Srilalitha Vinnakota, Development of benzo[b]thiophene linked-oxadiazole derivatives for potential antimicrobial and anti-TB targets: Evaluation of ADME-tox and *in-silico* docking, J. Adv. Chem. Sci. 12(5) (2026) 1021–1029.

2.2 Biological Evaluation

Antibacterial, antifungal and antitubercular activities of the title compounds (**7a–7k**) was assessed using a reported in agar well diffusion and microplate alamar blue assays (MABA) assay and the results are described as zone of inhibition and MIC values in Table 1. To evaluate the anti-microbial and antitubercular potential of the compounds, gemifloxacin and streptomycin were used as the reference drugs [44, 45]. The *in vitro* antibacterial and antifungal activities were screened by agar well diffusion technique against Gram-(+ve) bacteria: *Staphylococcus aureus, Streptococcus pyogenes*, Gram-(-ve) *Pseudomonas aeruginosa, Klebsiella pneumoniae*, and fungal strains: *Candida albicans, Aspergillus clavatus.* Gemifloxacin and Clotrimazole were employed as reference drugs for antibacterial and antifungal activity correspondingly. All the compounds displayed good to moderate activity with respect to diameter zone of inhibition values when compared to reference drug. The compounds **7a**, **7c**, **7f**, and **7h** were observed as the most potent antibacterial compounds with zone of inhibition (ZI) values ranging from 38.20 to 26.30 mm as compared to standard GMF (ZI=34.25 to 37.02 mm). From antibacterial screening results, compound **7a** showed excellent antibacterial activity on the *P. aeruginosa*, *K. pneumoniae*, *S. aureus*, and *S. pyogenes* strains with ZI values 34.38±1.06, 33.70±2.02, 26.30±1.30, and 28.90±0.62 mm, respectively. Specifically, compounds **7c** and **7f** showed promising antibacterial effects against *K. pneumoniae*, and *S. pyogenes*, with ZI values of 35.62±0.84, 33.68±1.39, 38.20±2.25, and 35.20±0.66 mm, respectively. Likewise, compound **7h** displayed strongest bacterial against the *P. aeruginosa* and *S. pyogenes* microorganisms, with diameter zone values of 35.34±0.67, and 36.26±2.62 mm, respectively. Both compounds **7e**, **7i** and **7j** demonstrated activity comparable to or moderate than GMF, which are exhibited ZI values of 22.58±0.36, 17.47±0.52, and 23.20±1.19 mm against *Pseudomonas aeruginosa*, respectively. Also, these compounds showed moderate to less activities than GMF which are showed ZI values of 18.09±1.14, 15.23±2.02, and 13.51±1.37 mm against *Klebsiella pneumoniae*, respectively.

The results revealed that the highest antimicrobial potency is exhibited by the compounds **7c**, **7d,** and **7f** with zone of inhibition values of 27.67±2.06, 28.90±1.10, 39.95±0.82 mm on the Gram-(+ve) *S. aureus* strain and compared to GMF (37.02±0.92 mm). Additionally, compounds **7h** (ZI=27.57±2.36 µg/mL) and **7j** (ZI=22.45±1.22 mm) also showed significant antimicrobial activity on the *S. aureus* microorganism (Fig. 1).

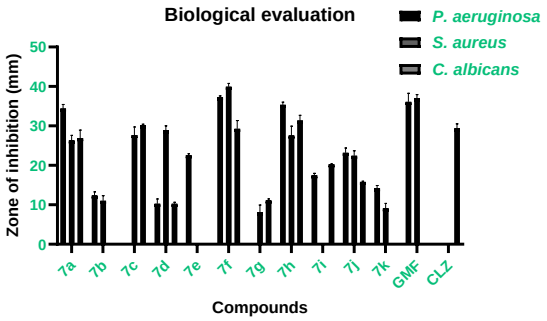

Fig. 1 Visual antibacterial and antifungal sensitivity of final oxadiazole analogues (**7a-7k**)

The other derivatives have week antibacterial activity with the ZI range values (8.12±1.80–11.01±1.32 mm, whereas, **7e**, and **7i** did not showed activity on the *S. aureus*. The prepared *bis*-oxadiazole analogues **7a**, **7c**, **7f**, and **7h** displayed potent antifungal activity against *C. albicans* having zone of inhibition values 26.90±2.02, 30.15±0.28, 29.28±2.09, 31.37±1.32 mm and compared to CLZ (ZI=29.36±1.15 mm). In addition, benzo[*b*]thiophene derivatives **7i** and **7j** had shown moderate activity with zone of inhibition of 20.26±0.08, 15.83±0.15 mm, whereas compounds **7d**, and **7g** were found to be less active on the fungal strain *C. albicans*. The antifungal activity of synthesized compounds **7c**, **7e** and **7j** revealed as the most potent compounds (ZI 28.10±0.32, 19.36±0.26, 18.45±1.16 for *A. clavatus* respectively) as compared to standard drug CLZ (ZI=27.23±1.54 mm). The prepared oxadiazoles 7**d**, **7g** and **7i** showed moderate antifungal activity against *A. clavatus* (ZI 14.10±0.18, 15.10±0.25, and 12.09±0.20 mm), while the compound **7a, 7f** and **7h** have not showed antifungal activity against *A. clavatus*.

The antitubercular activity results demonstrated a diverse range of activities among the synthesized compounds. The most potent TB-effects were observed with compounds **7a**, **7c**, **7f** and **7h** exhibiting excellent activity on $H_{37}Rv$ strain. Specifically, compounds **7f** and **7h** showed promising antitubercular effects against $H_{37}Rv$ strain, with MIC values of 2.89, and 3.10 µM, respectively, when compared to streptomycin (STM) (MIC= 3.25 µM) (Fig. 2).

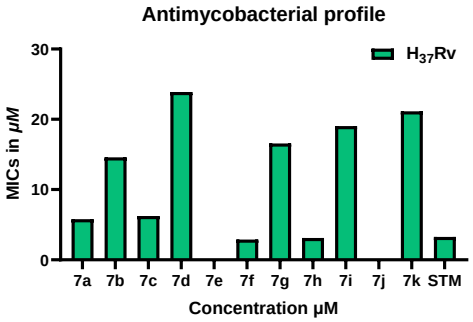

Fig. 2 Graphical representation of anti-TB MIC concentrations of synthesized compounds (**7a-7k** and **STM**)

Likewise, compound **7a** and **7c** displayed strong anti-TB activity against the same $H_{37}Rv$ strain, with MIC values of 5.80, and 6.23 µM, respectively. Both compounds **7b** and **7g** demonstrated activity comparable to or moderate than STM, which exhibited MIC values of 14.58, and 16.56 µM against $H_{37}Rv$, respectively. Also, the prepared analogues **7d** and **7k** showed less anti-TB activities which showed MIC values of 23.89, and 21.13 µM against $H_{37}Rv$ strain, respectively. The electron donating strongly activating methyl group in compound **7c** may be responsible for better antimicrobial and anti-tubercular potency. The presence of weakly deactivating electron withdrawing nitro and chloro groups present in compound **7k** and **7b** have less antimicrobial and anti-TB activity. With regards to the prepared analogues (**7a-7k**), their ZI/MIC were either equal to or two times less than the corresponding ZI/MIC. Overall, from the antimicrobial/TB activity study it can be concluded that the synthesized analogues having hydroxy/chloro substitution on the 3rd position of aromatic ring are utmost active amongst all the derivatives.

2.3 Docking Analysis

The potential of the newly created ligand (**7h**) to activate the *Candida albicans* active site from the 5FSA protein was examined using sterol 14-alpha demethylase (CYP51) from a pathogenic yeast. We were able to acquire the protein molecules from the RCSB Protein Data Bank [46–49] and two strong ligands (**7c** and **7f**) were permitted for docking studies using the DprE1 complex with the CT325-hexagonal crystal form of *Mycobacterium* TB (PDB ID: 4FDN). The most popular technique for calculating protein-ligand interactions is molecular docking, which is also an effective way to forecast possible ligand interactions. To ensure that powerful ligands have an inhibitory mechanism, molecular docking was used. This study significantly advances our understanding of molecular biological profiles. We carried out a molecular docking investigation on strong compounds that, according to biological evaluation, were the best inhibitors. Using the Autodock4.2 binding free energy/dissociation constant assessment to determine the optimal binding conformation, the native compounds in this investigation have been identified as antitubercular and antifungal protein inhibitors. According to the docking results, ligand molecules engage in several interactions with the enzymes in order to attach to the active site (Table 2, Figs. 3-5). Ligands **7c**, **7f**, and **7h**, with their respective negative scoring energy values of –11.77, –10.68, and –9.16 kcal. mol^{-1}, produced the most stable combination with the *M. tuberculosis* and *C. albicans* targets.

After, docking results of compound **7c** with *M. TB* protein suggested the formation of the hydrogen bond (H-bond) between 1,2,4-oxadiazole and Gly77(A) at a distance 2.67 Å. Additionally, this ligand has been stabilized by residues such as Gly^{199}(A), Ile^{203}(A), Gly^{202}(A), Met^{94}(A), Thr^{142}(A), Gly^{137}(A), Lys^{438}(A), Tyr^{80}(A), Leu^{76}(A), and Gly^{75}(A) *via* hydrophobic week van der Waals forces. The binding orientation of the 1,2,3-triazole core exhibited two backbone H-bondings with Ser^{79}(A) (2.94 Å), and Arg^{78}(A) (2.68 Å) within the catalytic active site of *M. TB*. The graphical inspection afforded better details of the compound **7c** which established three π-sigma bondings, one π-sigma bond between 1,3,4-oxadiazole with Val^{141}(A) (3.56 Å), second π-sigma bond with benzo[*b*]thiophene and Ile^{151}(A) (3.23 Å) and another π-sigma interaction between mesityl and Ala^{73}(A) (3.02 Å) active site residues, as shown in Fig. 3. The molecule is stabilized by π-alkyl & alkyl-alkyl residues such as Ile^{204}(A), Ala^{148}(A), Ala^{84}(A) x 2, Arg^{74}(A), Ala^{73}(A), Ile^{151}(A), Pro^{136}(A) x 2, Ala^{437}(A) x 3, Arg^{78}(A), and Val^{141}(A). This compound also exhibited two non-polar π-π interactions with the gatekeeper residue Gly^{144}(A), His^{152}(A) at a distance

https://doi.org/10.30799/jacs.280.26120501

Cite this Article as: Nagaraju Madala, Vishal Sharma, Srilalitha Vinnakota, Development of benzo[b]thiophene linked-oxadiazole derivatives for potential antimicrobial and anti-TB targets: Evaluation of ADME-tox and *in-silico* docking, J. Adv. Chem. Sci. 12(5) (2026) 1021–1029.

3.26, and 3.53 Å respectively. Additionally, the benzo[*b*]thiophene core formed one hydrophobic π-donor H-bond interaction with Tyr^{435}(A) in the hinge region, along with one carbon hydrogen (CH) bond with Gly^{145}(A). π–π interaction between aromatic structures or sigma–π interactions between the positively charged portions of the ligand and aromatic surfaces in the protein have been observed. These interactions favour the localization and stability of the ligand at apolar sites in the binding pocket.

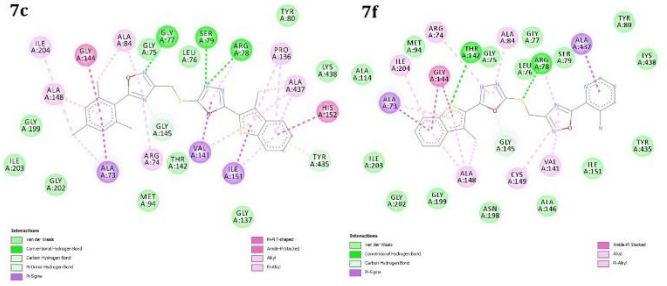

Fig. 3 Visual representation of the 2D complex *M. tuberculosis* mutant [4FDN]

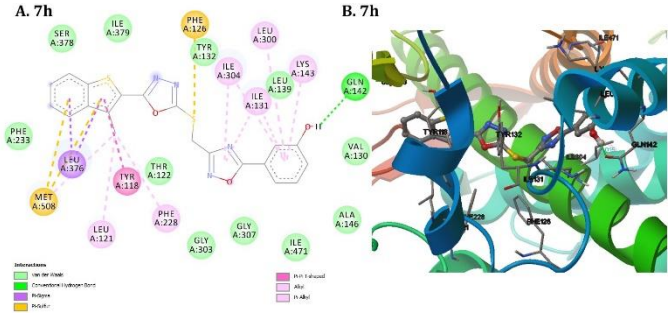

Fig. 4 Visual representations of the 2D and 3D-complexs of *C. albicans* mutant [5FSA]

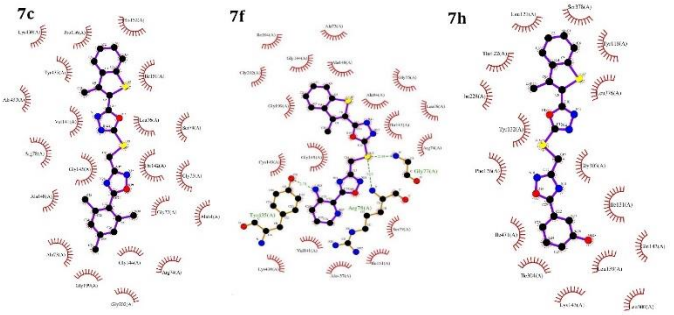

Fig. 5 Ligplot docking confirmations of most active compounds **7c**, **7f** and **7h**

Compound **7f** exhibited a binding energy of −10.68 kcal. mol^{-1} and a dissociation constant 308.17 nM. Within the *M. TB* domain, its benzo[*b*]thiophene moiety established one H-bond with Thr^{142}(A) (2.90 Å) and sulphur linker showed one more H-bond with Arg^{78}(A) (3.02 Å). The central 1,3,4-oxadiazole core contributed to CH-bond interaction with Gly^{145}(A) at distance of 2.45 Å. Additionally, the benzo[*b*]thiophene moiety formed two hydrophobic π-π stackings with Gly^{144}(A) in the hinge region. Within the benzo[*b*]thiophene and pyridin-3-amine motifs area of compound **7f** engaged in two π-sigma stackings and five π-alkyl electrostatic interactions with Ala^{73}(A), Ala^{437}(A), Ile^{204}(A), Ala^{73}(A), and Ala^{148}(A) x 3 residues respectively. After assessment of best docking pose of second most potent compound (**7f**) it was found to form fifteen van der Waals bonds among Ala^{114}(A), Ile^{203}(A), Gly^{202}(A), Gly^{199}(A), Asn^{198}(A), Ala^{146}(A), Ile^{151}(A), Tyr^{435}(A), Lys^{438}(A), Tyr^{80}(A), Ser^{79}(A), Leu^{76}(A), Gly^{77}(A), Gly^{75}(A), and Met^{94}(A) with benzo[*b*]thiophene, oxadiazole and pyridin-3-amine groups (Fig. 3). The NH_2 group of terminal pyridine ring established backbone H-bond with Tyr^{435}(A) at an inter-plane distance of ~ 2.71 Å (Fig. 5).

The amino acid residues in the 5FSA-Compound **7h** interaction show that the *meta*-hydroxy phenyl group connected to the hydrogen atom forms a hydrogen bond with Gln^{142}(A) residue at distance (2.72 Å). Amino acids with π-sigma and π-sulfur hydrophobic side chains such as Leu376(A) and Met508(A) are shown to interact with the ligand. Such interactions play a critical role in ligand localization to the protein. 1,2,4-Oxadiazole and *meta*-hydroxy phenyl units appeared as embedded in a large π-alkyl hydrophobic pocket framed by Met^{508}(A), Ile^{304}(A) x 2, Ile^{131}(A) x 2, Leu^{300}(A), and Lys^{143}(A) (Fig. 4). Interactions such as π-π stacking attraction between benzo[*b*]thiophene and the negatively charged Tyr^{118}(A), this ligand plays an important role in ligand binding. The van der Waal bonds formation by Phe^{233}(A), Ser^{378}(A), Ile^{379}(A), Thr^{122}(A), Tyr^{132}(A), Leu^{139}(A), Val^{130}(A), Ala^{146}(A), Ile^{471}(A), Gly^{307}(A), Gly^{303}(A), and Thr^{122}(A) residues indicates that the ligand is specifically stabilized with the 5FSA protein, and these bonds may play an important role. The interactions can increase its binding affinity and these bonds contribute to the binding stability of the ligand.

2.4 ADME-Tox Analysis

Using *in silico* simulations of membrane permeability, biomolecular interactions during absorption and excretion, and structural stability throughout the metabolic process, computational methods have become more popular in recent years for analyzing and forecasting ADME features. The target compounds' chemical structures were first sketched in ChemBioDraw Ultra 14.0 for this investigation, and their SMILES notations were taken out for additional computer analysis. SwissADME and ADMET lab3.0, two important prediction systems, were then used to process these SMILES strings. As reputable online servers, http://www.swissadme.ch/ and https://admetlab3.scbdd.com/server/screening conducted studies on drug likeness evaluation and ADME-T prediction of the produced compounds **7a-7k** and reference substance streptomycin [50–53]. Tables 3 and 4 provide a list of the collected data. All synthesized compounds meet the Lipinski Rule of Five, Pfizer Rule, Golden Triangle, and their molecular descriptors, including LogP, molecular weight (MW), hydrogen bond acceptor (HBA), hydrogen bond donor (HBD), and topological polar surface area (TPSA), fall within the acceptable range for drug-like properties, according to an evaluation of the data in Tables 3, 4 and Fig. 7. Total surface is a measure of the number of polar atoms. It is said to be related to passive molecule transport through membranes, which enables the computation of drug transport properties in the intestines and blood–brain barrier transit. Furthermore, Veber *et al*. state that analogues with a TPSA of ≤ 140 Å^2 and rotatable bonds of ≤ 10 are presumed to have great bioavailability. A ligand that has the most rotatable bonds is more flexible and may be adjusted to interact with the active site cavity more effectively. Compounds (**7a–7k**) in the current study showed a satisfactory drug-like profile, indicating improved oral bioavailability. It is anticipated that the selected analogues will have strong oral bioavailability because they are situated above the pink region zone on the bioavailability radar map, which considers the following characteristics. The target range of physicochemical space (LIPO: lipophilicity, SIZE: MWt, POLAR: TPSA, INSOLU: solubility, INSATU: Insaturation, and FLEX: flexibility) is shown by the pink area in the radar graphic (Fig. 6). The degree of insolubility and insaturation for compounds **7c** and **7i** is the sole property that significantly deviates from its ideal value.

Fig. 6 Bioavailability radar plot form of **7c, 7i** and **STM**

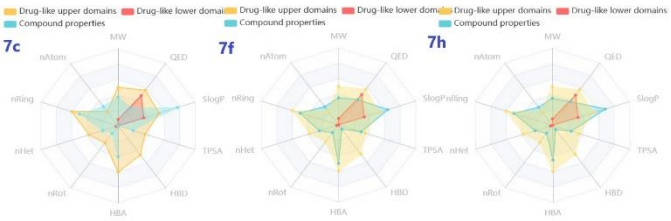

Fig. 7 Bioavailability radar plot form of **7c, 7i** and **STM**

The novel target compounds fall into one of two categories: either they are non-toxic for the liver, or H-HT negative, with a value of 0 to 0.3 (green/excellent), or they are toxic for the liver, or H-HT positive, with a predicted value of 0.3 to 0.7 (yellow/medium) for moderate toxicity and 0.7 to 1.0 (red/poor) for strong toxicity. As a result, compounds **7c** and **7d** are classified as significant carcinogens and showed medium projected values of 0.593 and 0.744 respectively. The other derivatives, with expected ranges of 0.771–0.901, are classified as poor carcinogens. These days, the metabolism prediction model has focused on how target substances interact with cytochromes P450 monooxygenase enzymes (CYP1A2, CYP3A4, CYP2C19, and CYP2D6) which are concentrated in the

https://doi.org/10.30799/jacs.280.26120501

Cite this Article as: Nagaraju Madala, Vishal Sharma, Srilalitha Vinnakota, Development of benzo[b]thiophene linked-oxadiazole derivatives for potential antimicrobial and anti-TB targets: Evaluation of ADME-tox and *in-silico* docking, J. Adv. Chem. Sci. 12(5) (2026) 1021–1029.

liver and catalysed the phase 1 metabolism of pharmaceuticals. One of the main mechanisms causing pharmacokinetic drug-drug interactions is the inhibition of cytochromes enzymes. Table 3 shows that all bis-oxadiazoles **7a–7k** based on benzo[b]thiophene were predicted to be non-inhibitors on three different enzymes CYP1A2, CYP2C19, CYP2D6, whereas these were predicted to inhibit the CYP3A4 enzyme. Furthermore, while the remaining compounds are all oxadiazoles, compounds **7j** and **7k** may not be suitable substrates for P-glycoprotein (Pgp). Furthermore, all of the compounds had low GI absorption since they were situated in the grey part of the egg, because they were situated close to the white part of the egg. Lastly, none of the benzo[*b*]thiophene-*bis*-oxadiazoles found in boiled egg yolks were able to cross the blood–brain barrier (Fig. 8).

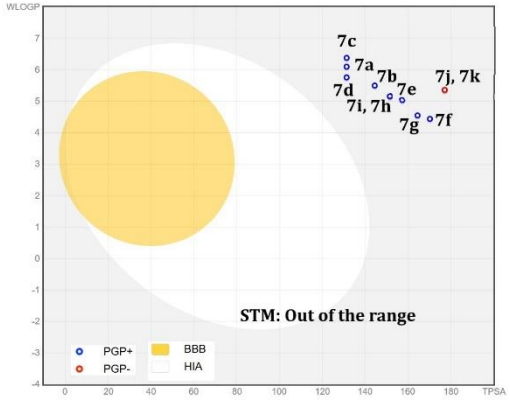

Fig. 8 BOILED-Egg predictive for the final *bis*-oxadiazole analogues

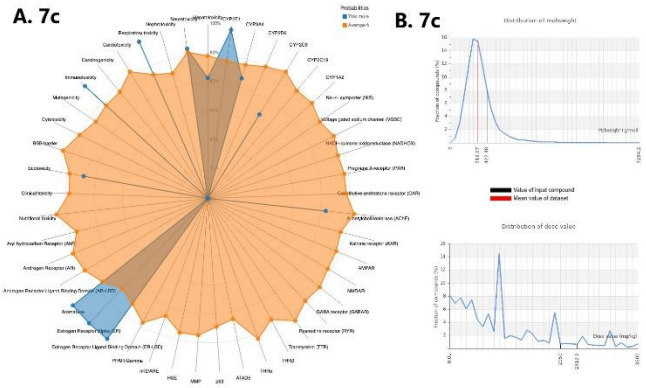

Fig. 9 A). The toxicity radar chart of oxadiazole **7c**. B). Comparison of input compound (**7c**) with dataset compound

All of the target compounds **7a–7k** have strong passive AMES permeabilities, ranging from 0.044 to 0.916 cm s^{-1}, as shown in Table 4. With projected values of over 90% (range from 99.67% to 101.78%), it can be inferred from the information above that the oxadiazole associated with benzo[*b*]thiophene (**7a–7k**) has a high interaction with plasma protein. Furthermore, these substances might only have a marginal membrane-crossing efficiency and a low therapeutic index. The best-docked oxadiazoles, according to our research, demonstrated suitable physio-chemical, pharmacokinetic, and bioavailability in silico without any toxicity or carcinogenicity (Fig. 9), suggesting that they might be a promising new class of antitubercular/antimicrobial drugs.

Table 1 [a]Antibacterial/antifungal potency expressed as ZI (mm) of final *bis*-oxadiazole scaffolds. [b]Antitubercular activity expressed as MICs (μM) of benzo[*b*]thiophene derivatives on the $H_{37}Rv$

Entry	[a]Bactericidal activity [Zone of inhibition in mm] ± SD				Antifungal profiles [Zone of inhibition in mm] ± SD		[b]Anti-TB Activity [MIC in μM]
	Gram-(-ve) strains		Gram-(+ve) strains		List of the fungal strains		Strain
	P. aeruginosa	*K. pneumoniae*	*S. aureus*	*S. pyogenes*	*C. albicans*	*A. clavatus*	*$H_{37}Rv$*
7a	34.38±1.06	33.70±2.02	26.30±1.30	28.90±0.62	26.90±2.02	NA	5.80
7b	12.34±0.95	7.20±1.13	11.01±1.32	9.35±1.22	NA	10±1.45	14.58
7c	NA	35.62±0.84	27.67±2.06	38.20±2.25	30.15±0.28	28.10±0.32	6.23
7d	10.27±1.20	14.57±1.55	28.90±1.10	27.90±1.35	10.28±0.36	14.10±0.18	23.89
7e	22.58±0.36	18.09±1.14	NA	16.72±1.26	NA	19.36±0.26	> 25
7f	37.29±0.33	33.68±1.39	39.95±0.82	35.20±0.66	29.28±2.09	NA	2.89
7g	NA	26.12±0.06	8.12±1.80	NA	11.10±0.37	15.10±0.25	16.56
7h	35.34±0.67	NA	27.57±2.36	36.26±2.62	31.37±1.32	NA	3.10
7i	17.47±0.52	15.23±2.02	NA	15.83±1.42	20.26±0.08	12.09±0.20	19.04
7j	23.20±1.19	13.51±1.37	22.45±1.22	NA	15.83±0.15	18.45±1.16	> 25
7k	14.20±0.68	NA	9.09±1.26	17.14±1.30	NA	13.03±0.05	21.13
GMF[c]	36.10±2.17	34.70±0.85	37.02±0.92	34.25±0.39	ND	ND	ND
CLZ[d]	ND	ND	ND	ND	29.36±1.15	27.23±1.54	ND
STM[e]	ND	ND	ND	ND	ND	ND	3.25

[c]GMF: Gemifloxacin, [d]CLZ: Clotrimazole, [e]STM: Streptomycin, ZI (mm): 35–50 (very strong), 21–35 (strong), 11–20 (moderate), and 1–10 (weak). MIC (μM): 1–5 (very strong), 5–10 (strong), 10–20 (moderate), and 20–25 (weak). NA: not active; ND: not done; Each value is an average of three replicates, ± denotes standard deviation among triplicates. The activity analysis of each compound was performed three times; > 25 μM: not active

Table 2 Interaction analysis of new *bis*-oxadiazoles with 4FDN and 5FSA

Ligands	Docking energy	Dissociation constant	Hydrophobic amino acid residues	H-bond amino acid residues
M. tuberculosis DprE1 complex with 4FDN				
7c	−11.77 kcal. mol^{-1}	3.72 μM	Van der Waals: Gly^{199}(A), Ile^{203}(A), Gly^{202}(A), Met^{94}(A), Thr^{142}(A), Gly^{137}(A), Lys^{438}(A), Tyr^{80}(A), Leu^{76}(A), Gly^{75}(A) π-alkyl & alkyl: Ile^{204}(A), Ala^{148}(A), Ala^{84}(A) x 2, Arg^{74}(A), Ala^{73}(A), Ile^{151}(A), Pro^{136}(A) x 2, Ala^{437}(A) x 3, Arg^{78}(A), Val^{141}(A) π-sigma: Ala^{73}(A), Val^{141}(A), Ile^{151}(A); π-π stacked: Gly^{144}(A), His^{152}(A) CH-bond: Gly^{145}(A); π-donor H-bond: Tyr^{435}(A)	Gly^{77}(A), Ser^{79}(A), Arg^{78}(A)
7f	−10.68 kcal. mol^{-1}	308.17 nM	Van der Waals: Ala^{114}(A), Ile^{203}(A), Gly^{202}(A), Gly^{199}(A), Asn^{198}(A), Ala^{146}(A), Ile^{151}(A), Tyr^{435}(A), Lys^{438}(A), Tyr^{80}(A), Ser^{79}(A), Leu^{76}(A), Gly^{77}(A), Gly^{75}(A), Met^{94}(A); π-alkyl & alkyl: Ile^{204}(A), Ala^{73}(A), Arg^{74}(A), Ala^{84}(A), Ala^{148}(A) x 3, Cys^{149}(A), Val^{141}(A), Arg^{78}(A); π-sigma: Ala^{73}(A), Ala^{437}(A) π-π stacked: Gly^{144}(A) x 2; CH-bond: Gly^{145}(A)	Thr^{142}(A), Arg^{78}(A), Tyr^{435}(A), Gly^{77}(A)
Sterol 14α-demethylase (CYP51) from antifungal pathogenic yeast *C. albicans* [5FSA]				
7h	−9.16 kcal. mol^{-1}	192.21 nM	Van der Waals: Phe^{233}(A), Ser^{378}(A), Ile^{379}(A), Thr^{122}(A), Tyr^{132}(A), Leu^{139}(A), Val^{130}(A), Ala^{146}(A), Ile^{471}(A), Gly^{307}(A), Gly^{303}(A), Thr^{122}(A) π-alkyl & alkyl: Met^{508}(A), Leu^{121}(A), Phe^{228}(A), Ile^{304}(A) x 2, Ile^{131}(A) x 2, Leu^{300}(A), Lys^{143}(A); π-π stacked: Tyr^{118}(A) π-sigma: Leu^{376}(A); π-sulfur: Met^{508}(A) x 2, Phe^{126}(A)	Gln^{142}(A)

https://doi.org/10.30799/jacs.280.26120501

Cite this Article as: Nagaraju Madala, Vishal Sharma, Srilalitha Vinnakota, Development of benzo[b]thiophene linked-oxadiazole derivatives for potential antimicrobial and anti-TB targets: Evaluation of ADME-tox and *in-silico* docking, J. Adv. Chem. Sci. 12(5) (2026) 1021–1029.

Table 3 Physicochemical and pharmacokinetics properties of final *bis*-oxadiazole compounds (**7a-7k**)

S.No	Csp^3	nRot	nHA	nHD	TPSA	iLogp	Log S (Watersol.)	GI absor.	BBB Perm.	P-gp sub.	CYP 1A2 inh.	CYP2C19	CYP 2D6	CYP 3A4
7a	0.10	5	6	0	77.84	4.40	-6.48	Low	No	Yes	No	No	No	Yes
7b	0.11	5	7	0	90.73	3.95	-6.04	Low	No	Yes	No	No	No	Yes
7c	0.22	5	6	0	77.84	4.59	-6.78	Low	No	Yes	No	No	No	Yes
7d	0.14	5	6	0	77.84	4.49	-6.19	Low	No	Yes	No	No	No	Yes
7e	0.10	5	6	1	103.86	3.59	-5.53	Low	No	Yes	No	No	No	Yes
7f	0.11	5	7	1	116.75	3.44	-4.89	Low	No	Yes	No	No	No	Yes
7g	0.11	5	8	1	110.96	3.32	-5.10	Low	No	Yes	No	No	No	Yes
7h	0.10	5	7	1	98.07	3.79	-5.75	Low	No	Yes	No	No	No	Yes
7i	0.10	5	7	1	98.07	3.65	-5.75	Low	No	Yes	No	No	No	Yes
7j	0.10	6	8	0	120.98	3.63	-5.93	Low	No	No	No	No	No	Yes
7k	0.10	6	8	0	120.98	3.58	-5.93	Low	No	No	No	No	No	Yes
STM	0.86	9	15	12	336.43	-0.06	2.18	Low	No	Yes	No	No	No	No

Table 4 Medicinal chemistry and toxicity properties of final prepared oxadiazole scaffolds (**7a-7k**)

S.No	hERG	H-HT	AMES	Skin Sen	Carcinogen.	Eye Irrita.	SA score	NP score	Lipi. Rule	Pfizer Rule	Golden Tri.	PPB	$T_{1/2}$
7a	0.008	0.799	0.056	0.403	0.903	0.035	2.582	-2.40	Yes	Yes	Yes	101.77	0.045
7b	0.005	0.834	0.073	0.237	0.906	0.044	2.793	-2.201	Yes	Yes	Yes	101.30	0.061
7c	0.002	0.593	0.091	0.329	0.913	0.061	2.756	-1.936	Yes	Yes	Yes	101.57	0.044
7d	0.006	0.744	0.096	0.399	0.908	0.055	2.529	-2.223	Yes	Yes	Yes	101.30	0.052
7e	0.006	0.863	0.087	0.136	0.914	0.087	2.617	-2.103	Yes	Yes	Yes	100.76	0.055
7f	0.005	0.901	0.219	0.22	0.888	0.071	2.83	-2.115	Yes	Yes	Yes	99.67	0.098
7g	0.014	0.847	0.066	0.172	0.888	0.044	2.807	-2.032	Yes	Yes	Yes	100.25	0.152
7h	0.011	0.777	0.044	0.227	0.898	0.095	2.641	-1.889	Yes	Yes	Yes	101.00	0.147
7i	0.007	0.771	0.058	0.204	0.903	0.116	2.598	-1.918	Yes	Yes	Yes	101.09	0.126
7j	0.069	0.89	0.916	0.438	0.914	0.09	2.644	-2.329	Yes	Yes	Yes	101.78	0.053
7k	0.084	0.886	0.897	0.443	0.907	0.071	2.677	-2.397	Yes	Yes	Yes	101.77	0.066
STM	0.142	0.329	0.067	0.024	0.009	0.001	5.678	1.772	No	Yes	No	20.43	0.183

0-0.1 (---), 0.1-0.3 (--) [🟢: excellent]; 0.3-0.5 (-), 0.5-0.7(+), [🟡: medium]; 0.7-0.9 (++), and 0.9-1.0 (+++) [🔴: poor]

Table 5 Prediction of Toxicity of active compounds by using Protox-II

Targets	Prediction/Probability		
	7c	**7f**	**7h**
Hepatotoxicity	Active/0.60	Active/0.63	Active/0.63
Neurotoxicity	Inactive/0.51	Active/0.52	Inactive/0.60
Nephrotoxicity	Inactive/0.54	Inactive/0.58	Inactive/0.50
Respiratory toxicity	Active/0.61	Active/0.69	Active/0.63
Cardiotoxicity	Inactive/0.83	Inactive/0.86	Inactive/0.76
Carcinogenicity	Active/0.51	Active/0.68	Active/0.50
Immunotoxicity	Inactive/0.99	Inactive/0.99	Inactive/0.96
Mutagenicity	Active/0.56	Active/0.56	Active/0.54
Cytotoxicity	Inactive/0.86	Inactive/0.84	Inactive/0.79
BBB-barrier	Active/0.87	Active/0.82	Active/0.72
Clinical toxicity	Inactive/0.56	Inactive/0.56	Inactive/0.55
Androgen Receptor (AR)	Inactive/0.91	Inactive/0.95	Inactive/0.92
Estrogen Receptor Alpha (ER)	Inactive/0.75	Inactive/0.77	Inactive/0.82
GABA receptor	Inactive/0.78	Inactive/0.79	Inactive/0.83
Pregnane X receptor	Inactive/0.65	Inactive/0.77	Inactive/0.71

3. Experimental Methods

3.1 Materials and Methods

All chemicals and reagents, listed in the supplementary data, were purchased from Sigma-Aldrich and Merck were used without further purification. Reactions were monitored by thin-layer chromatography (TLC) silica gel plates containing, performed on silica gel glass plates containing 60 GF-254. Melting points were measured using a 9200 electrothermal melting point apparatus and are presented without correction. ^{1}H NMR and ^{13}C NMR spectra were recorded using Bruker 400 MHz and 100 MHz spectrophotometer. Chemical shifts (δ) are reported in parts per million relatives to tetramethylsilane (TMS) as the internal reference, while coupling constants (J) are given in hertz. The signal patterns are denoted as singlet (s), doublet (d), doublet of doublets (dd), triplet (t), and multiplet (m). Mass spectra and elemental analyses were recorded on Shimadzu Qp-2010 plus spectrometer.

3.2 Synthesis of Intermediate Compound 5

As described in Scheme 1, 1-(2-chlorophenyl)ethan-1-one (**1**) (5.0g, 32.46 mmol), methyl 2-mercaptoacetate (5.16g, 48.70 mmol) and sodium hydride (2.33g, 97.40 mmol) were stirred jointly into *N, N*-dimethyl formamide (50 mL) and the reaction was monitored at refluxing temperature for 3 h. After completion the reaction followed by evaporation of the solvent, then washing with acetone, to obtain the cyclised product (white solid, yield: 80%). The remaining intermediate compounds, up to **4** were prepared by using the previous literature [40] and used for further reaction without purification.

*3.3 Synthesis of 2-((5-(3-Methylbenzo[b]thiophen-2-yl)-1,3,4-oxadiazol-2-yl)thio)acetonitrile (**5**)*

As described in Scheme 2, A solution of 5-(3-methylbenzo[*b*]thiophen-2-yl)-1,3,4-oxadiazole-2-thiol (**4**) (4.0g, 16.12 mmol) and potassium carbonate (2.5g, 20.96 mmol) was prepared in acetone (40 mL) and was stirred for 15 min. Then, 2-bromoacetonitrile (2.49g, 20.96 mmol) was added at below rt for 20 min, and the reaction mixture was refluxed for 6 h. The purity of the product was determined by TLC, the solvent system used was n-hexane: ethyl acetate (8:2). The reaction mixture was filtered and washed with dichloromethane/water, and the solvent were evaporated under reduced pressure. The obtained product was purified by flash column chromatography using hexane: ethyl acetate (8:2) to give the brownish product **5** (88%, 112-114 °C).

https://doi.org/10.30799/jacs.280.26120501

Cite this Article as: Nagaraju Madala, Vishal Sharma, Srilalitha Vinnakota, Development of benzo[b]thiophene linked-oxadiazole derivatives for potential antimicrobial and anti-TB targets: Evaluation of ADME-tox and *in-silico* docking, J. Adv. Chem. Sci. 12(5) (2026) 1021–1029.

*3.4 Preparation of (Z)-N'-hydroxy-2-((5-(3-methylbenzo[b]thiophen-2-yl)-1,3,4-oxadiazol-2-yl)thio)acetimidamide (**6**)*

2-((5-(3-methylbenzo[*b*]thiophen-2-yl)-1,3,4-oxadiazol-2-yl)thio)acetonitrile (**5**) (3.5g, 12.19 mmol) in dichloromethane (35 mL) was reacted with hydroxylamine hydrochloride (1.7g, 24.39 mmol) for half an hour at rt. Subsequently, triethylamine (2.46g, 24.39 mmol) was introduced to the reaction mixture, and after an instant reaction the contents were stirred for 10 hours. The progress of the reaction was monitored by thin-layer chromatography (TLC) [n-hexane: ethyl acetate (8:2)]. The light brownish colour solid product was formed in a reaction mixture. Upon completion, the solvent was removed and the crude product was washed with water and filtered and recrystallization from ethanol to yield the light brownish solid (83% yields, mp. 168-170 °C).

*3.5 General Procedure for the Preparation of Benzo[b]thiophene-1,3,4-oxadiazole Linked to 1,2,4-Oxadiazole Molecules (**7a-7k**)*

Acetimidamide **6** (3.0g, 9.37 mmol), EDC.HCl (2.14g, 11.25 mmol) and the corresponding acid (*m*-chlorobenzoic acid) (2.19g, 14.06 mmol) were charged in 30 mL of DCM at 15 °C in a three-necked flask for the experiment, and it was agitated for 3–4 hours at reflux temperature. Then, the acylated intermediate was refluxing in the presence of sodium acetate (0.92g, 11.25 mmol) in ethanol for 4-5 h. Following TLC monitoring to verify acetimidamide **6** consumption (EtOAc: Hexane; 2:8). The reaction mixture was put into 100 mL of dil. $NaHCO_3$, brine solution (50 mL) and 150 mL of DCM before being moved into a separating funnel. Anhydrous Na_2SO_4 was used to dry the organic phase before it was filtered. After the target compound was purified using flash column chromatography, the solvent was extracted under vacuum, enabling its recovery.

3.6 Spectroscopic Data

*3.6.1 5-(3-Chlorophenyl)-3-(((5-(3-methylbenzo[b]thiophen-2-yl)-1,3,4-oxadiazol-2-yl)thio)methyl)-1,2,4-oxadiazole **(7a)***

Yield 80%, White solid, mp 229 °C. ^{1}H-NMR spectrum (DMSO–d_6, 400 MHz), *δ*, ppm: 2.27 s (3H, Ar-CH_3), 4.57 s (2H, SCH_2), 7.42-7.52 m (4H, Ar-H), 7.61 d (1H, *J*=8.6 Hz, Ar-H), 7.83-7.91 t (2H, *J*=9.2 Hz, Ar-H), 8.02 *s* (1H, Ar-H). ^{13}C NMR spectrum (DMSO-d_6, 100 MHz), δ_C, ppm: 15.8, 35.5, 119.6, 122.8, 125.2, 126.5, 128.8, 130, 132.2, 135.3, 136.4, 138.2, 141.2, 142.4, 143.5, 159.2, 162.4, 176.2. Mass spectrum, *m/z*: 441.0310 $[M+H]^+$, 442.0504 $[M+2H]^+$. Elemental analysis: Calculated, C 54.48; H 2.97; Cl 8.04; N 12.71; S 14.54. $C_{20}H_{13}ClN_4O_2S_2$. Found, C 54.37; H 2.88; Cl 7.95; N 12.60; S 14.43.

*3.6.2 5-(6-Chloropyridin-2-yl)-3-(((5-(3-methylbenzo[b]thiophen-2-yl)-1,3,4-oxadiazol-2-yl)thio) methyl)-1,2,4-oxadiazole **(7b)***

Yield 72%, Brownish solid, mp 210 °C. ^{1}H-NMR spectrum (DMSO–d_6, 400 MHz), *δ*, ppm: 2.28 s (3H, Ar-CH_3), 4.52 s (2H, SCH_2), 7.31 d (1H, *J*=8.6 Hz, Ar-H), 7.44 t (1H, *J*=9.2 Hz, Ar-H), 7.63-7.68 m (2H, Ar-H), 7.91 d (1H, *J*=8.6 Hz, Ar-H), 8.30 t (1H, *J*=9.2 Hz, Ar-H), 8.48 d (1H, *J*=8.6 Hz, Ar-H). ^{13}C NMR spectrum (DMSO-d_6, 100 MHz), δ_C, ppm: 14.8, 35.7, 120.5, 125, 126, 129.1, 130.7, 131.6, 132.5, 139.2, 141.6, 142.4, 144.4, 149.3, 157.3, 159.2, 162.4, 164.8. Mass spectrum, *m/z*: 442.9865 $[M+H]^+$, 443.9798 $[M+2H]^+$. Elemental analysis: Calculated, C 51.73; H 2.84; Cl 8.12; N 15.94; S 14.61. $C_{19}H_{12}ClN_5O_2S_2$. Found, C 51.64; H 2.74; Cl 8.02; N 15.85; S 14.51.

*3.6.3 5-Mesityl-3-(((5-(3-methylbenzo[b]thiophen-2-yl)-1,3,4-oxadiazol-2-yl)thio)methyl)-1,2,4-oxadiazole (**7c**)*

Yield 73%, White solid, mp 192 °C. ^{1}H-NMR spectrum (DMSO–d_6, 400 MHz), *δ*, ppm: 2.18 s (3H, Ar-CH_3), 2.32 s (3H, Ar-CH_3), 2.70 s (6H, Ar-CH_3), 4.50 s (2H, SCH_2), 7.03 s (1H, Ar-H), 7.42 t (1H, *J*=9.2 Hz, Ar-H), 7.59 t (1H, *J*=9.2 Hz, Ar-H), 7.74 d (1H, *J*=8.6 Hz, Ar-H), 7.93 d (1H, *J*=8.6 Hz, Ar-H). ^{13}C NMR spectrum (DMSO-d_6, 100 MHz), δ_C, ppm: 14.8, 18.9, 22.7, 36.1, 120.3, 122.7, 125, 126, 126.5, 129.1, 132, 136.2, 137.2, 139.6, 141.2, 142.5, 144.8, 159.8, 162.4, 175.7. Mass spectrum, *m/z*: 449.0477 $[M+H]^+$. Elemental analysis: Calculated, C 61.67; H 4.57; N 12.57; S 14.37. $C_{23}H_{20}N_4O_2S_2$. Found, C 61.58; H 4.48; N 12.48; S 14.27.

*3.6.4 3-(((5-(3-Methylbenzo[b]thiophen-2-yl)-1,3,4-oxadiazol-2-yl)thio) methyl)-5-(p-tolyl)-1,2,4-oxadiazole **(7d)***

Yield 70%, Off-white solid, mp 185 °C. ^{1}H-NMR spectrum (DMSO–d_6, 400 MHz), *δ*, ppm: 2.19 s (3H, Ar-CH_3), 2.34 s (3H, Ar-CH_3), 4.47 s (2H, SCH_2), 7.28 d (2H, *J*=8.0 Hz, Ar-H), 7.49 t (1H, *J*=9.2 Hz, Ar-H), 7.60 t (1H, *J*=9.2 Hz, Ar-H), 7.77 d (1H, *J*=8.6 Hz, Ar-H), 7.90 d (1H, *J*=8.6 Hz, Ar-H), 8.11 d (2H, *J*=8.0 Hz, Ar-H). ^{13}C NMR spectrum (DMSO-d_6, 100 MHz), δ_C, ppm: 15.2, 21.2, 36.4, 121.6, 124.2, 125, 126.2, 127.2, 129.2, 130.6, 132.9, 136.3, 141.2, 142.8, 145.6, 161.2, 162.7, 178.9. Mass spectrum, *m/z*: 421.8810 $[M+H]^+$. Elemental analysis: Calculated, C 59.97; H 3.83; N 13.31; S 15.24. $C_{21}H_{16}N_4O_2S_2$. Found, C 59.86; H 3.72; N 13.19; S 15.15.

*3.6.5 4-(3-(((5-(3-Methylbenzo[b]thiophen-2-yl)-1,3,4-oxadiazol-2-yl)thio) methyl)-1,2,4-oxadiazol-5-yl)aniline (**7e**)*

Yields 76%, Light brown solid; mp: 176 °C; ^{1}H-NMR spectrum (DMSO–d_6, 400 MHz), *δ*, ppm: 2.32 s (3H, Ar-CH_3), 4.45 s (2H, SCH_2), 5.45 brs (2H, NH_2), 6.68 d (2H, *J*=8.0 Hz, Ar-H), 7.43 t (1H, *J*=9.2 Hz, Ar-H), 7.52 t (1H, *J*=9.2 Hz, Ar-H), 7.74 d (2H, *J*=8.0 Hz, Ar-H), 8.01 d (1H, *J*=8.6 Hz, Ar-H), 8.18 d (1H, *J*=8.6 Hz, Ar-H). ^{13}C NMR spectrum (DMSO-d_6, 100 MHz), δ_C, ppm: 14.3, 33.7, 114, 115.7, 120.7, 122.7, 125.8, 128.2, 129.8, 132.1, 139.7, 141.4, 142.6, 146.8, 159.7, 162.3, 176.9. Mass spectrum, *m/z*: 422.4275 $[M+H]^+$. Elemental analysis: Calculated, C 56.98; H 3.58; N 16.61; S 15.20. $C_{20}H_{15}N_5O_2S_2$. Found, C 56.87; H 3.46; N 16.51; S 15.09.

*3.6.6 2-(3-(((5-(3-Methylbenzo[b]thiophen-2-yl)-1,3,4-oxadiazol-2-yl)thio) methyl)-1,2,4-oxadiazol-5-yl)pyridin-3-amine (**7f**)*

Yields 81%, Brown solid; mp: 194 °C; ^{1}H-NMR spectrum (DMSO–d_6, 400 MHz), *δ*, ppm: 2.29 s (3H, Ar-CH_3), 4.41 s (2H, SCH_2), 5.70 brs (2H, NH_2), 7.16 d (1H, *J*=8.6 Hz, Ar-H), 7.29 t (1H, *J*=9.2 Hz, Ar-H), 7.41 t (1H, *J*=9.2 Hz, Ar-H), 7.85 d (1H, *J*=8.6 Hz, Ar-H), 8.08 d (1H, *J*=8.6 Hz, Ar-H), 8.23 d (1H, *J*=8.6 Hz, Ar-H). ^{13}C NMR spectrum (DMSO-d_6, 100 MHz), δ_C, ppm: 14.4, 35.1, 122.5, 124.3, 126, 128.8, 131, 135.1, 136.4, 137.6, 141.7, 142.7, 145.1, 157.9, 163.7, 167.6. Mass spectrum, *m/z*: 423.1281 $[M+H]^+$. Elemental analysis: Calculated, C 54.12; H 3.43; N 19.97; S 15.26. $C_{19}H_{14}N_6O_2S_2$. Found, C 54.02; H 3.34; N 19.89; S 15.18.

*3.6.7 6-(3-(((5-(3-Methylbenzo[b]thiophen-2-yl)-1,3,4-oxadiazol-2-yl)thio) methyl)-1,2,4-oxadiazol-5-yl)pyridin-3-ol (**7g**)*

Yields 76%, Brown solid; mp: 202 °C; ^{1}H-NMR spectrum (DMSO–d_6, 400 MHz), *δ*, ppm: 2.21 s (3H, Ar-CH_3), 4.47 s (2H, SCH_2), 7.41-7.51 m (3H, Ar-H), 7.70 d (1H, *J*=8.6 Hz, Ar-H), 7.90 d (1H, *J*=8.6 Hz, Ar-H), 8.22 d (1H, *J*=8.6 Hz, Ar-H), 8.34 s (1H, Ar-H), 10.25 brs (1H, OH). ^{13}C NMR spectrum (DMSO-d_6, 100 MHz), δ_C, ppm: 14.5, 35, 118.1, 119.4, 120.4, 123, 125.6, 125.7, 129, 131.5, 137, 137.9, 149.1, 157.6, 163.2, 164.4, 165.9. Mass spectrum, *m/z*: 424.0627 $[M+H]^+$. Elemental analysis: Calculated, C 53.88; H 3.08; N 16.53; S 15.13. $C_{19}H_{13}N_5O_3S_2$. Found, C 53.77; H 3.01; N 16.42; S 15.04.

*3.6.8 3-(3-(((5-(3-Methylbenzo[b]thiophen-2-yl)-1,3,4-oxadiazol-2-yl)thio) methyl)-1,2,4-oxadiazol-5-yl)phenol (**7h**)*

Yield 64%, Off-white solid, mp 175 °C. ^{1}H-NMR spectrum (DMSO–d_6, 400 MHz), *δ*, ppm: 9.59 brs (1H, OH), 8.09 d (1H, *J*=8.6 Hz, Ar-H), 7.92 d (1H, *J*=8.6 Hz, Ar-H), 7.71 d (1H, *J*=8.6 Hz, Ar-H), 7.48 t (1H, *J*=9.2 Hz, Ar-H), 7.32 d (1H, *J*=8.6 Hz, Ar-H), 7.21 t (1H, *J*=9.2 Hz, Ar-H), 7.02 s (1H, Ar-H), 6.74 d (1H, *J*=8.6 Hz, Ar-H), 4.29 s (2H, SCH_2), 2.37 s (3H, Ar-CH_3). ^{13}C NMR spectrum (DMSO-d_6, 100 MHz), δ_C, ppm: 14.6, 35.6, 111.9, 115.3, 120.1, 122, 123.2, 124.8, 127.6, 127.7, 128.9, 131.5, 138.6, 139, 142.8, 157.8, 158, 162.3, 176.8. Mass spectrum, *m/z*: 423.0656 $[M+H]^+$. Elemental analysis: Calculated, C 56.85; H 3.33; N 13.25; S 15.17. $C_{20}H_{14}N_4O_3S_2$. Found, C 56.74; H 3.24; N 13.14; S 15.08.

*3.6.9 4-(3-(((5-(3-Methylbenzo[b]thiophen-2-yl)-1,3,4-oxadiazol-2-yl)thio) methyl)-1,2,4-oxadiazol-5-yl)phenol (**7i**)*

Yield 60%, Off-white solid, mp 170 °C. ^{1}H-NMR spectrum (DMSO–d_6, 400 MHz), *δ*, ppm: 2.23 s (3H, Ar-CH_3), 4.33 s (2H, SCH_2), 6.90 d (2H, *J*=8.0 Hz, Ar-H), 7.28 t (1H, *J*=9.2 Hz, Ar-H), 7.38 t (1H, *J*=9.2 Hz, Ar-H), 7.61 d (1H, *J*=8.6 Hz, Ar-H), 7.81 d (2H, *J*=8.0 Hz, Ar-H), 7.98 d (1H, *J*=8.6 Hz, Ar-H), 9.82 brs (1H, OH). ^{13}C NMR spectrum (DMSO-d_6, 100 MHz), δ_C, ppm: 14.2, 34.1, 116.2, 119.3, 120.4, 122.6, 125.9, 126.8, 129.3, 130.5, 140.6, 141.9, 162, 162.8, 163.9, 176.1. Mass spectrum, *m/z*: 423.1481 $[M+H]^+$. Elemental analysis: Calculated, C 56.94; H 3.42; N 13.33; S 15.03. $C_{20}H_{14}N_4O_3S_2$. Found, C 56.85; H 3.33; N 13.25; S 15.17.

*3.6.10 3-(((5-(3-Methylbenzo[b]thiophen-2-yl)-1,3,4-oxadiazol-2-yl)thio) methyl)-5-(4-nitrophenyl)-1,2,4-oxadiazole (**7j**)*

Yield 78%, Yellow solid, mp 210 °C. ^{1}H-NMR spectrum (DMSO–d_6, 400 MHz), *δ*, ppm: 2.30 s (3H, Ar-CH_3), 4.39 s (2H, SCH_2), 7.35 t (1H, *J*=9.2 Hz, Ar-H), 7.50 t (1H, *J*=9.2 Hz, Ar-H), 7.61 d (1H, *J*=8.6 Hz, Ar-H), 7.82 d (1H,

https://doi.org/10.30799/jacs.280.26120501

Cite this Article as: Nagaraju Madala, Vishal Sharma, Srilalitha Vinnakota, Development of benzo[b]thiophene linked-oxadiazole derivatives for potential antimicrobial and anti-TB targets: Evaluation of ADME-tox and *in-silico* docking, J. Adv. Chem. Sci. 12(5) (2026) 1021–1029.

J=8.6 Hz, Ar-H), 8.32 d (2H, *J*=8.0 Hz, Ar-H), 8.62 d (2H, *J*=8.0 Hz, Ar-H). ^{13}C NMR spectrum (DMSO-d_6, 100 MHz), δ_C, ppm: 14.9, 34.6, 120.1, 123.5, 124.5, 128.2, 128.6, 129.9, 134.7, 135.5, 137.5, 142.4, 143.8, 148.2, 157.7, 160.1, 175.5. Mass spectrum, *m/z*: 452.0316 $[M+H]^+$. Elemental analysis: Calculated, C 53.21; H 2.90; N 15.51; S 14.20. $C_{20}H_{13}N_5O_4S_2$. Found, C 53.11; H 2.80; N 15.41; S 14.10.

*3.6.11 3-(((5-(3-Methylbenzo[b]thiophen-2-yl)-1,3,4-oxadiazol-2-yl)thio) methyl)-5-(3-nitrophenyl)-1,2,4-oxadiazole (**7k**)*

Yield 72%, Yellow solid, mp 221 °C. ^{1}H-NMR spectrum (DMSO–d_6, 400 MHz), δ, ppm: 2.35 s (3H, Ar-CH_3), 4.31 s (2H, SCH_2), 7.32 t (1H, *J*=9.2 Hz, Ar-H), 7.43 t (1H, *J*=9.2 Hz, Ar-H), 7.75 d (1H, *J*=8.6 Hz, Ar-H), 7.86 t (1H, *J*=9.2 Hz, Ar-H), 7.88 d (1H, *J*=8.6 Hz, Ar-H), 8.29 d (1H, *J*=8.6 Hz, Ar-H), 8.40 d (1H, *J*=8.6 Hz, Ar-H), 8.51 s (1H, Ar-H). ^{13}C NMR spectrum (DMSO-d_6, 100 MHz), δ_C, ppm: 14.3, 33.6, 120.3, 121.8, 122.7, 123.4, 124, 125.1, 129.6, 131.1, 139.2, 140.9, 142.3, 146.7, 159.7, 161.1, 176.9. Mass spectrum, *m/z*: 452.4855 $[M+H]^+$. Elemental analysis: Calculated, C 53.31; H 2.98; N 15.60; S 14.29. $C_{20}H_{13}N_5O_4S_2$. Found, C 53.20; H 2.89; N 15.50; S 14.20. Experimental section of biological evaluation, docking protocol and the structures of these compounds were determined using analytical methods including NMR (^{1}H/^{13}C), and HRMS spectrometry.

4. Conclusion

This study aimed to investigate the antimicrobial/anti-TB potential of benzo[b]thiophene-based bis-oxadiazole derivatives (**7a–7k**) using an integrated approach in good yields that combined *in vitro* biological assays with computational analysis. The recently synthesized benzo[*b*]thiophene analogues were characterized through ^{1}H/^{13}C-NMR, IR and HRMS spectroscopy. These compounds were tested for their *in vitro* antibacterial activity on *S. aureus, S. pyogenes*, *P. aeruginosa,* and *K. pneumoniae* and antifungal potency against *C. albicans* and *A. clavatus.* Compound **7a**, **7c**, **7f**, and **7h** were the most potent antibacterial oxadiazole molecules and showed ZI values ranging from 26.30 to 38.20 mm, compared to GMF, with ZI values of 34.25 to 37.02 mm, respectively. Specifically, compounds **7c** and **7f** showed promising antibacterial effects against *K. pneumoniae*, and *S. pyogenes*, with ZI values of 35.62±0.84, 33.68±1.39, 38.20±2.25, and 35.20±0.66 mm, respectively. The anti-TB results of the compounds **7f**, and **7h** exhibited the potent activity against the H_{37}Rv strain, with MIC values 2.89 and 3.10 µM, respectively, these two compounds showed greater activity than the reference drug STM. In fact, the ligand-**7h** had the most negative ΔG (−9.16 kcal. mol^{-1}) that showed favourable hydrophobic, H-bond, and CH-bond interactions with the key amino acid residues at active site of *C. albicans* receptor (PDB: 5FSA). *In-silico* ADME/Tox profiling showed favorable pharmacokinetic properties for compounds **7a–7k**, complying with Lipinski's Rule of Five and demonstrating promising oral bioavailable drugs. These findings provide a solid foundation for further biological evaluation and structure optimization towards the development of novel antimicrobial therapeutics.

Acknowledgement

One of the authors (NM) is thankful to Medicinal Chemistry Division, VSN LABS, IDA Cherlapally, Hyderabad, India and JNTUH University for providing the required facilities and motivation for the completion of the research work.

References

[1] G.K. Sandhu, Tuberculosis: current situation, challenges and overview of its control programs in India, J. Glob. Infect. Dis. 3(2) (2011) 143–150.
[2] C.F. McQuaid, A. Vassall, T. Cohen, K. Fiekert, R.G. White, The impact of COVID-19 on TB: a review of the data, Int. J. Tuberc. Lung Dis. 25(6) (2021) 436–446.
[3] K. Dheda, F. Mirzayev, D.M. Cirillo, Z. Udwadia, K.E. Dooley, et al., Tuberculosis, Nat. Rev. Dis. Primers 10 (2024) 22.
[4] S. Mukherjee, S. Perveen, A. Negi, R. Sharma, Evolution of tuberculosis diagnostics: from molecular strategies to nanodiagnostics, Tuberculosis 140 (2023) 102340.
[5] S. Bagcchi, WHO's Global Tuberculosis Report 2022, Lancet Microbe 4 (2023) e20.
[6] S.H. Alotaibi, Study of drug interaction, mutant frequency and mutant prevention concentration of DFMBT against *Mycobacterium tuberculosis* H37Rv, Microb. Pathog. 176 (2023) 106023.
[7] S. Doron, S.L. Gorbach, Bacterial infections: overview, in: H.K. Heggenhougen (Ed.), International Encyclopedia of Public Health, Academic Press, Oxford, 2008, pp.273–282.
[8] C.J.L. Murray, K.S. Ikuta, F. Sharara, L. Swetschinski, G.R. Aguilar, et al., Global burden of bacterial antimicrobial resistance in 2019: a systematic analysis, Lancet 399 (2022) 629–655.
[9] R. Lucas, Y. Hadizamani, J. Gonzales, B. Gorshkov, T. Bodmer, et al., Impact of bacterial toxins in the lungs, Toxins 12(4) (2020) 223.
[10] M.A. Salam, M.Y. Al-Amin, M.T. Salam, J.S. Pawar, N. Akhter, et al., Antimicrobial resistance: A growing serious threat for global public health, Healthcare (Basel). 11 (2023) 1946.
[11] R. Kaur, P. Rani, A.G. Atanasov, Q. Alzahrani, R. Gupta, et al., Discovery and development of antibacterial agents: fortuitous and designed, Mini Rev. Med. Chem. 22 (2022) 984–1029.
[12] J.S. Lim, Y.Y. Chai, W.X. Ser, A. Van Haeren, Y.H. Lim, et al., Novel drug candidates against antibiotic-resistant microorganisms: a review, Iran. J. Basic Med. Sci. 27 (2024) 134–150.
[13] J. Ramírez-Prada, Synthesis of novel quinoline-based 4,5-dihydro-1H-pyrazoles as potential anticancer, antifungal, antibacterial and antiprotozoal agents, Eur. J. Med. Chem. 131 (2017) 237–254.
[14] S. Kumar, S. Gupta, V. Rani, P. Sharma, Pyrazole containing anti-HIV agents: an update, Med. Chem. 18 (2022) 831–846.
[15] Y. Ogawa, E. Tokunaga, O. Kobayashi, K. Hirai, N. Shibata, Current contributions of organofluorine compounds to the agrochemical industry, iScience 23 (2020) 101467.
[16] R. Dua, R. Dua, S. Shrivastava, S.K. Sonwane, S.K. Srivastava, Pharmacological significance of synthetic heterocycles scaffold: a review, Adv. Biol. Res. 5 (2011) 120–144.
[17] E. Kabir, M. Uzzaman, A review on biological and medicinal impact of heterocyclic compounds, Results Chem. 4 (2022) 100606.
[18] P.K. Sharma, T. Qadir, A. Amin, D. Sarkar, Synthesis of medicinally important indole derivatives: a review, Open Med. Chem. J. 15(1) (2021) 1–16.
[19] F. Liu, J. Hu, L. Chang, Y. Jiang, In vitro anti-mycobacterial activity of novel benzo[c]thiophene-1,3-dione: a novel scaffold against *Mycobacterium tuberculosis*, Microb. Pathog. 148 (2020) 104466.
[20] G. Naganagowda, B. Padmashali, Utility of 3-chlorobenzothiophene-2-carbonyl isothiocyanate for the synthesis of some novel biheterocycles of expected biological activity, Phosphorus Sulfur Silicon Relat. Elem. 185 (2010) 1369–1380.
[21] E. Pinto, M.J.R.P. Queiroz, L.A. Vale-Silva, J.F. Oliveira, A. Begouin, et al., Antifungal activity of synthetic di(hetero)arylamines based on the benzo[b]thiophene moiety, Bioorg. Med. Chem. 16 (2008) 8172–8177.
[22] S. Pathak, A.P. Singh, R. Sharma, R. Pandey, An overview of the pharmacological activities and synthesis of benzothiophene derivatives, Med. Chem. 20(9) (2024) 839–854.
[23] R.S. Keri, K. Chand, S. Budagumpi, B.S. Somappa, S.A. Patil, et al., An overview of benzo[b]thiophene-based medicinal chemistry, Eur. J. Med. Chem. 138 (2017) 1002–1033.
[24] N.R. Penthala, V.N. Sonar, J. Horn, M. Leggas, J.S. Yadlapalli, et al., Synthesis and evaluation of a series of benzothiophene acrylonitrile analogs as anticancer agents, MedChemComm 4 (2013) 1073–1078.
[25] W.W. Wardakhan, O.M. Abdel-Salam, G.A. Elmegeed, Screening for antidepressant, sedative and analgesic activities of novel fused thiophene derivatives, Acta Pharm. 58 (2008) 1–14.
[26] T.S. Ibrahim, A.J. Almalki, A.H. Moustafa, R.M. Allam, G.E.-D.A. Abuo-Rahma, et al., Novel 1,2,4-oxadiazole-chalcone/oxime hybrids as potential antibacterial DNA gyrase inhibitors: design, synthesis, ADMET prediction and molecular docking study, Bioorg. Chem. 111 (2021) 104885.
[27] P.K. Deb, N.A. Al-Shar'i, K.N. Venugopala, M. Pillay, P. Borah, In vitro anti-TB properties, in silico target validation, molecular docking and dynamics studies of substituted 1,2,4-oxadiazole analogues against *Mycobacterium tuberculosis*, J. Enzyme Inhib. Med. Chem. 36 (2021) 869–884.
[28] A.B. Reddy, T.R. Allaka, V.S.R. Avuthu, P.V.V.N. Kishore, H. Nagarajaiah, Imidazole-oxadiazole hybrids as potential antimicrobial agents: design, synthesis, drug-likeness, pharmacophore and molecular docking study, ChemistrySelect 9(32) (2024) e202401989.
[29] V.R. Yenireddy, A. Vejendla, Synthesis, characterization, biological evaluation and molecular docking of novel amide derivatives of indole-1,2,4-oxadiazole clubbed thiazoles, Chem. Data Collect. 39 (2022) 100861.
[30] B. Kulkarni, K. Manjunatha, M.N. Joy, A.M. Sajith, S. Santra, et al., Exploration of NMI-MsCl mediated amide bond formation for the synthesis of novel 3,5-substituted-1,2,4-oxadiazole derivatives: synthesis, evaluation of anti-inflammatory activity and molecular docking studies, Mol. Divers. 27 (2023) 1867–1878.
[31] A. Cherkasova, R. Astolfi, M. Nawrozkij, B. Gladkikh, E. Proia, et al., 1,2,4-Oxadiazoles in medicinal chemistry: trends of the last years, Eur. J. Med. Chem. 297 (2025) 117935.
[32] T.M. Dhameliya, S.J. Chudasama, T.M. Patel, B.P. Dave, A review on synthetic account of 1,2,4-oxadiazoles as anti-infective agents, Mol. Divers. 26 (2022) 2967–2980.
[33] Salahuddin, M.A. Yar, R. Mazumder, G.S. Chakraborthy, M.J. Ahsan, et al., Updates on the synthesis and biological activities of 1,3,4-oxadiazole: a review, Synth. Commun. 47 (2017) 1805–1847.
[34] S. Gandamalla, S. Mavurapu, K. Sambaru, T.R. Allaka, Substituted 1,3,4-oxadiazole coupled 1,2,3-triazole derivatives as antiproliferative agents: design, synthesis, biological evaluation and in silico studies, J. Chin. Chem. Soc. 72(6) (2025) 721–738.
[35] A.B. Reddy, V.S.R. Avuthu, P.V.V.N. Kishore, T.R. Allaka, H. Nagarajaiah, New triazole-based oxadiazolo/thiadiazolo-phthalazines as potent antimycobacterial agents: design, synthesis, molecular modelling and in silico ADMET profiles, ChemistrySelect 9 (2024) e202304020.
[36] G.V. Rao, T.R. Allaka, M.K. Gandla, P.K. Veera Venkata Nanda, S.R. Pindi, et al., Synthesis, antimicrobial activity and in silico studies of fluoroquinolones

https://doi.org/10.30799/jacs.280.26120501

Cite this Article as: Nagaraju Madala, Vishal Sharma, Srilalitha Vinnakota, Development of benzo[b]thiophene linked-oxadiazole derivatives for potential antimicrobial and anti-TB targets: Evaluation of ADME-tox and *in-silico* docking, J. Adv. Chem. Sci. 12(5) (2026) 1021–1029.

bearing 1,3,4-oxadiazolyl-triazole derivatives, J. Heterocycl. Chem. 60(10) (2023) 1666–1683.
[37] N. Shajari, P. Eskandari, A comprehensive overview of the recent development of privileged 1,3,4-oxadiazole derivatives and their biological activities, J. Mol. Struct. 1349 (2026) 143639.
[38] A. Husain, M. Ajmal, Synthesis of novel 1,3,4-oxadiazole derivatives and their biological properties, Acta Pharm. 59 (2009) 223–233.
[39] G.S. Desta, K. Balakrishna, Synthesis, characterization, biological evaluation, and molecular docking studies of new 1,3,4-oxadiazole-thioether derivative as antioxidants and cytotoxic agents, Heliyon 10 (2024) e28634.
[40] S.Z.B. Bohurudeen, A. Ambala, T.R. Allaka, M.Z. Ahmed, B. Thirunavukkarasu, et al., Novel benzothiophene-tethered 1,3,4-oxadiazoles as potent antimicrobial targets: design, synthesis, biological evaluation, DFT exploration and in silico docking study, J. Mol. Struct. 1322 (2025) 140251.
[41] R.G. Miriyala, J. Sannapaneni, P.R. Kanuparthy, V.R. Singamaneni, T.R. Allaka, et al., A new class of benzo[b]thiophene-1,3,4-oxadiazole bearing 1,2,4-oxadiazoles as potent antimicrobial targets: synthesis, biological evaluation, docking, DFT and ADMET studies, ChemistrySelect 11(3) (2026) e05667.
[42] T.R. Allaka, B. Kummari, N. Polkam, N. Kuntala, K. Chepuri, et al., Novel heterocyclic 1,3,4-oxadiazole derivatives of fluoroquinolones as potent antibacterial agents: synthesis and computational molecular modelling, Mol. Divers. 26 (2022) 1581–1596.
[43] S.C. Karad, V.B. Purohit, R.P. Thummar, B.K. Vaghasiya, R.D. Kamani, et al., Synthesis and biological screening of novel 2-morpholinoquinoline nucleus clubbed with 1,2,4-oxadiazole motifs, Eur. J. Med. Chem. 126 (2017) 894–909.
[44] C. Valgas, S.M. de Souza, E.F.A. Smânia Jr., Screening methods to determine antibacterial activity of natural products, Braz. J. Microbiol. 38 (2007) 369–380.
[45] S. Cho, H.S. Lee, S.G. Franzblau, Microplate Alamar Blue Assay (MABA) and Low Oxygen Recovery Assay (LORA) for *Mycobacterium tuberculosis*, Methods Mol. Biol. 1285 (2015) 281–292.
[46] S.M. Batt, T. Jabeen, V. Bhowruth, L. Quill, P.A. Lund, et al., Structural basis of inhibition of *Mycobacterium tuberculosis* DprE1 by benzothiazinone inhibitors, Proc. Natl. Acad. Sci. U.S.A. 109(28) (2012) 11354–11359.
[47] V. Gujja, K. Sadineni, M.R. Epuru, T.R. Allaka, V. Banothu, et al., Synthesis and in silico studies of some new 1,2,3-triazolyltetrazole bearing indazole derivatives as potent antimicrobial agents, Chem. Biodivers. 20(12) (2023) e202301232.
[48] T.Y. Hargrove, L. Friggeri, Z. Wawrzak, A. Qi, W.J. Hoekstra, et al., Structural analyses of *Candida albicans* sterol 14α-demethylase complexed with azole drugs address the molecular basis of azole-mediated inhibition of fungal sterol biosynthesis, J. Biol. Chem. 292(16) (2017) 6728–6743.
[49] A.K. Dunga, T.R. Allaka, Y. Kethavarapu, S.K. Nechipadappu, P. Pothana, et al., Design, synthesis and biological evaluation of novel substituted indazole-1,2,3-triazolyl-1,3,4-oxadiazoles: antimicrobial activity evaluation and docking study, Results Chem. 4 (2022) 100605.
[50] J. Dong, N.N. Wang, Z.J. Yao, L. Zhang, Y. Cheng, et al., ADMETlab: a platform for systematic ADMET evaluation based on a comprehensively collected ADMET database, J. Cheminform. 10 (2018) 29.
[51] G. Gogisetti, U. Kanna, V. Sharma, T.R. Allaka, B.R. Tadiboina, Design, synthesis and bio-evaluation of novel chalcones bridged with 1,3,4-oxadiazole linkers: ADMET and docking analysis, Chem. Biodivers. 19 (2022) e202200681.
[52] G. Xiong, Z. Wu, J. Yi, L. Fu, Z. Yang, et al., ADMETlab 2.0: an integrated online platform for accurate and comprehensive predictions of ADMET properties, Nucleic Acids Res. 49(W1) (2021) W5–W14.
[53] N. Muhamad, K. Na-Bangchang, The roles of CYP2C19 and CYP3A4 in the in vitro metabolism of β-eudesmol in human liver: reaction phenotyping and enzyme kinetics, Pharmacol. Res. Perspect. 11(6) (2023) e01149.

https://doi.org/10.30799/jacs.280.26120501

Cite this Article as: Nagaraju Madala, Vishal Sharma, Srilalitha Vinnakota, Development of benzo[b]thiophene linked-oxadiazole derivatives for potential antimicrobial and anti-TB targets: Evaluation of ADME-tox and *in-silico* docking, J. Adv. Chem. Sci. 12(5) (2026) 1021–1029.